Superradiant Emission Dynamics of an Optically Thin Material Sample in a Short-Decay-Time Optical Cavity

C. Greiner, B. Boggs, and T. W. Mossberg

Oregon Center for Optics and Department of Physics, University of Oregon, Eugene, Oregon 97403

(Received 10 May 2000)

We report observations of optical superradiant emission and the atomic evolution it drives under conditions closely approximating those originally envisioned in the classic work of Dicke [Phys. Rev. **93**, 99 (1954)]. Our experiment involves an optically thin solid sample in a short-lifetime optical cavity whose homogeneous coherence is cryogenically stabilized. Pulsed coherent excitation initiates superradiant emission which subsequently drives the sample to higher or lower states of coherence. Suppression of dephasing via cryogenics and propagation effects through use of an optically thin sample and cavity provides one of the clearest and cleanest examples of Dicke superradiance yet reported.

PACS numbers: 42.50.Fx, 42.50.Gy, 42.50.Md, 42.65.–k

In a classic paper [1] in 1954, Dicke showed that the spontaneous emission rate of a coherently radiating ensemble of N two-level atoms can substantially exceed that of N isolated atoms. He referred to those correlated multiatomic states exhibiting this abnormally large radiation rate as "superradiant states." To create a superradiant state Dicke originally proposed two methods: In the first, a completely inverted atomic ensemble is created that subsequently self-evolves to a superradiant state via initially incoherent spontaneous radiative coupling. In the second, a coherent radiation pulse directly excites the two-level atoms from the ground state to a superradiant state. Apparently, these methods lead to two basically distinct phenomena. In the first method atomic correlations develop spontaneously, initiated by incoherent spontaneous emission "noise" photons. This intrinsically quantum effect has been observed by several groups [2] in the 1970s and was later termed "superfluorescence" [3,4]. The second method is manifest in free-induction decay and certain other coherent transient phenomena [5] and is important since it alone allows for the deterministic preparation of selected superradiant states.

It has generally come to be believed that the optical thickness of a material is correlated with the maximal contribution that superradiant emission can make to the material's radiative energy relaxation. Specifically, optical thickness greater than unity is associated with strong superradiant damping [6]. To achieve high optical thickness it is usually necessary to work with spatially extended samples. However, the combination of large spatial extent and high optical thickness gives rise to propagation effects, e.g., superfluorescent ringing, that complicate the superradiant dynamics. Superfluorescent ringing is caused by energy transfer among longitudinal sample sections and is an intrinsic feature of propagation in media of high optical thickness [7]. While propagation effects are of fundamental importance they fall outside the description of superradiance originally given by Dicke. Being cooperative in nature, superradiant emission is suppressed by decohering effects of either homogeneous or inhomogeneous nature. Energy damping dominated by superradiant emission can occur only in environments with suitably small decoherence rates.

In the present manuscript, we demonstrate an experimental approach that provides for the study of classic Dicke superradiant emission free of many of the complications affecting previous work. In our experiment, an *optically thin* spatially extended material slab is placed within an optical cavity and directly prepared in a superradiant (not a fully inverted) state by pulsed excitation along the cavity axis. Since the sample is optically thin, excitation and emission fields remain essentially uniform throughout the sample length. While the spatial extent of our sample is larger than the emission wavelength, the phased-array excitation along the cavity axis eliminates propagational phase retardation effects in the manner implied in Dicke's original large sample model. The previous notion that strong superradiance requires optically thick samples is reflected in the large optical thickness of the (sample + cavity) composite system. To ensure atomic dynamics that are self-driven and use the cavity only for mediation of the superradiant field the empty-cavity ringdown time is chosen to be 3 orders of magnitude shorter than the operative superradiant emission time scale. In this limit, the cavity field is entirely determined by the material polarization. Still, the cavity acts to enhance the superradiant emission rate by a factor proportional to the cavity finesse. The observed cavity output provides a direct measure of the instantaneous sample polarization and its time evolution. Cavity and enclosed slab are cooled to liquid helium temperatures providing for a homogeneous material decoherence rate over an order of magnitude slower than the superradiant emission rate. Our observations provide the first comprehensive picture of emission dynamics, including material state evolution, that are clearly dominated by the superradiant field. In some instances we observe a postexcitation buildup of cavity emission

0031-9007/00/85(18)/3793(4)$15.00 © 2000 The American Physical Society

followed by decay indicating the sample's evolution toward and through a state of maximal cooperation under the influence of the superradiant emission process. Our approach to create superradiant states represents therefore an intriguing combination of Dicke's originally proposed methods as it involves both deterministic preparation and self-evolution to the maximally superradiant state.

Our work must be clearly distinguished from previous work involving atoms in cavities wherein the cavity coherence (energy storage) time was comparable or longer than the relevant radiative emission time [8]. In the case of slow cavity relaxation, energy oscillations back and forth between the cavity field and material excitation can occur. In the present instance, the cavity decay time is extremely fast compared to all other relevant rates and the energy stored in the cavity field is always orders of magnitude less than that stored in the material.

A schematic of our planospherical resonator and the sample is shown in Fig. 1. Mirror M1 (M2) has a radius of curvature of $R_1 = \infty$ ($R_2 = 10$ cm). Both mirrors have a reflectivity of 0.98 (± 0.01). The free spectral range of the cavity is measured to be $\sim$20 GHz, implying that the cavity's optical path length $L \approx 7.5$ mm. The minimum mode diameter ($1/e^2$ intensity points) is located at M1 and calculated to be $\sim$163 μm. The finesse and resonant transmission of the cavity—as measured outside the material absorption line—are $\mathcal{F} \approx 190$ and $\mathcal{T} \approx 54\%$, respectively. The finesse value indicates a mirror reflectivity slightly higher than nominal, while the lower than unity transmission indicates incomplete coupling of the input light to the fundamental cavity mode, unequal mirror reflectivities, or a combination. The cavity coherence time, deduced from the cavity line width, is $\tau_c \approx 1.5$ ns.

The sample employed is a 0.5-mm-thick slab of 0.1 at.% Tm^{3+}:YAG crystal. Tm^{3+} ions are excited on their $^3H_6(1)$-$^3H_4(1)$ absorption line. At $\sim$4.6 K, this transition has an inhomogeneous linewidth of $\sim$20 GHz, a decoherence time T_2 of 20 μs, an excited state ($^3H_4$) lifetime T_1 of $\sim$800 μs, and a center wavelength $\lambda_{\mathrm{Air}} \approx 793.17$ nm. Peak single pass sample absorption is measured to be $\sim$10%. Both facets of the crystal are antireflection coated ($R \leq 0.25\%$). The cavity increases the effective sample absorption by a factor proportional to the sample-modified small signal cavity finesse measured to be $\sim$23.

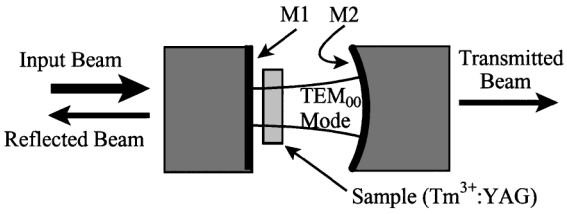

FIG. 1. Schematic of the cavity and sample. M1, cavity input mirror; M2, cavity output mirror.

Figure 2 is a schematic of the experimental setup. The output of an optically isolated external-cavity diode laser is gated by a series of two acousto-optic modulators (AOMs) to create excitation pulses with an on/off intensity contrast ratio of $\sim$80 dB and a rise time of $\sim$100 ns. An anamorphic prism pair and a pinhole are used to approximately circularize the elliptically shaped laser output to better match the fundamental cavity mode. For coupling into the cavity, the excitation pulse is focused to a focal spot of 150×180 μm^2 at input mirror M1. Both sample and cavity are cooled to $\sim$4.6 K. The transmission through cavity output mirror M2 is detected by a silicon avalanche photodiode. A beam splitter and a photodiode are used to monitor the excitation-pulse power.

In Fig. 3, we show the photodetected intensity transmitted through M2 versus time during and after sample excitation by a 2-μs-long excitation pulse. We note that only a narrow sub-MHz-wide portion of the sample's inhomogeneous linewidth is excited by the 2-μs pulse. The traces shown are averages of fifteen single-event traces. From the bottom to the top of Fig. 3, the excitation-pulse power P_{exc} is increased. Temporal boundaries of the excitation pulse are denoted by the sharp rising and falling edges. After the excitation field terminates, the cavity continues to emit for approximately 10 μs, about 4 orders of magnitude longer than the cavity damping time. The intensity and temporal structure of the output signal varies with P_{exc}. For the highest excitation-pulse intensity, the signal intensity builds up, peaks $\sim$0.5 μs after the end of the excitation pulse, and subsequently decreases. At the peak, the estimated intracavity Rabi frequency is about 120 kHz (assuming maximum orientational atom-field coupling [9]), implying that substantial atomic evolution driven by the superradiant emission takes place.

As pointed out by Dicke, the superradiant emission rate depends on the magnitude of the atomic coherence. For a homogeneously excited sample, it is maximum when the atoms are in a superposition of equal weights of ground and excited state and it decreases as the atoms are excited above or below this point. Inhomogeneous broadening

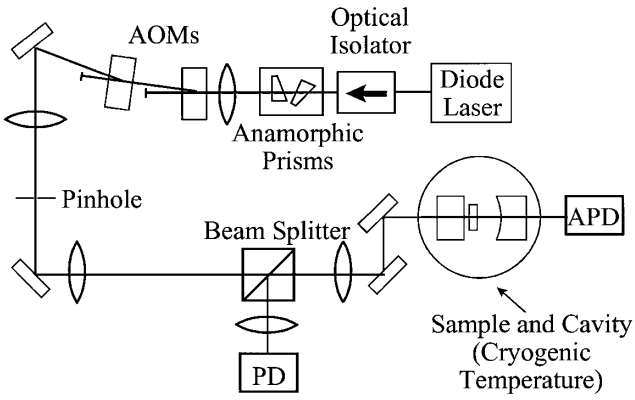

FIG. 2. Experimental setup: AOMs, acousto-optic modulators; APD, avalanche photodiode; PD, photodiode.

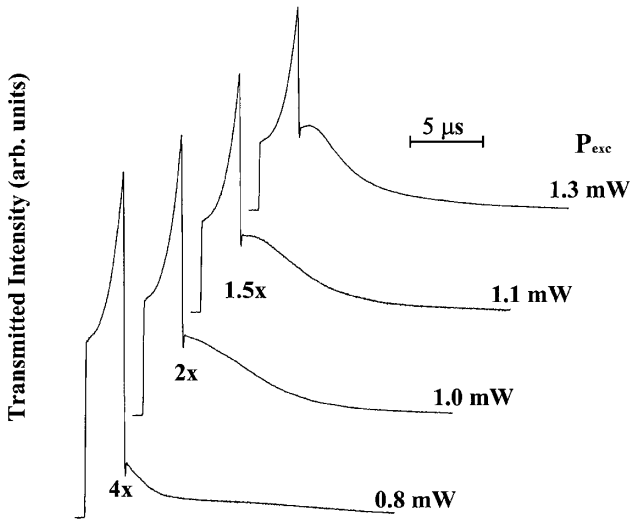

FIG. 3. Intensity transmitted through M2 versus time for different values of excitation power P_{exc}. The first 2 μs of the traces display the transmission of the excitation pulse, marked by the sharp rising and falling edges. The remainder of the traces corresponds to the superradiant emission signal.

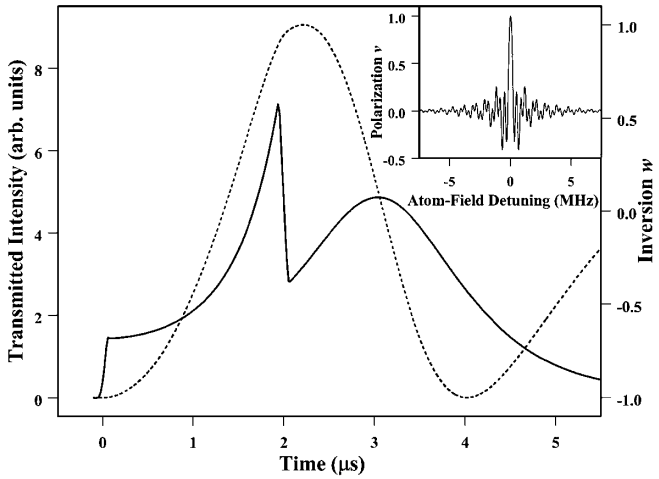

FIG. 4. Solid line, calculated transmitted intensity versus time, $0 < t < 2$ μs, excitation field on; dashed line, inversion w of resonant atoms versus time; inset, atomic polarization (Bloch vector ν component) versus detuning for $t = 3.1$ μs.

contributes additional richness to our experimental system, especially on time scales longer than the excitation-pulse duration. The interesting signal growth seen after excitation (top trace in Fig. 3) occurs on a time scale where inhomogeneous dephasing effects are relatively small. Simulation results, detailed below, indicate that maximum superradiant emission still occurs and is primarily caused by *resonant* atoms as they evolve through the half-inverted state.

We model our system using the coupled Maxwell-Bloch equations accounting for inhomogeneous broadening. We assume a 2-μs-long rectangular excitation pulse with a rise time of 100 ns and a uniform transverse intensity profile. The excitation field and cavity are resonant at the center frequency of the inhomogeneous absorption profile. The single-pass optical thickness of the sample, αL, is set to 0.1. Homogeneous atomic relaxation is neglected ($T_1 = T_2 = \infty$). Simulation cavity parameters match experimental ones. No intracavity loss mechanisms other than atomic absorption and mirror transmission are assumed. Figure 4 shows the calculated cavity transmission (solid line) approximately matching the topmost experimental trace of Fig. 3. The peak intracavity Rabi frequency of the superradiant field is $\sim$300 kHz. Shown as a dashed line is the inversion w of those atoms that are located at a cavity antinode and are resonant with the excitation field. Maximum superradiant emission occurs simultaneously with the evolution of these resonant atoms through $w = 0$ at $t = 3.1$ μs. In the inset we show the atomic polarization (Bloch vector ν component) versus detuning (from the excitation field) for the time of peak superradiant emission ($t = 3.1$ μs). The primary contribution to superradiant emission at the delayed emission peak stems from coherent atoms within a spectral bandwidth comparable to the excitation-pulse bandwidth. Note that the inversion of the resonant atoms continues to grow even after the excitation field has terminated. Also, and interestingly, the resonant atoms are reexcited for $t \geq 4$ μs. Our simulations indicate that the sustained inversion growth at $t \geq 2$ μs and the reexcitation for $t \geq 4\mu$s occur because of cavity-mediated energy transfer from detuned atoms. Under certain excitation conditions—to be detailed in a future publication—this effect leads to ringing in the superradiant cavity emission similar in behavior but of fundamentally different origin than the ringing phenomenon observed in Ref. [7]. Note that the long-term reexcitation phenomenon predicted does not cloud short-time superradiant behavior.

It is interesting to ask how efficiently superradiant emission depletes the energy injected into the sample by the excitation field. Under the simulation conditions of Fig. 4 the reradiated energy fraction $\eta = E_{\text{SR}}/E_{\text{abs}} \approx 0.59$, where E_{SR} (E_{abs}) is the energy emitted in the superradiant signal (absorbed from the excitation field). Less than unity reemission results primarily from inhomogeneous dephasing. For the uppermost trace in Fig. 3, we estimate $\eta \approx 0.15$; i.e., a substantial fraction of absorbed energy is emitted in the directional superradiant emission. Several factors reduce the fractional reemission below the calculated value. They are the following: (1) the excitation pulse has a nonuniform transverse intensity profile causing absorptive and diffractive loss from the cavity mode; (2) homogeneous atomic decohering is not entirely negligible on the emission time scale, since $T_2 \approx 20$ μs, and (3) the $^3H_6(1)$-$^3H_4(1)$ transition has multiple dipole moment orientations [9] making the atom-field coupling coefficient multivalued. It is nevertheless clear that superradiant emission, strong in the sense of fractional energy depletion, is being observed and that it self-coherently

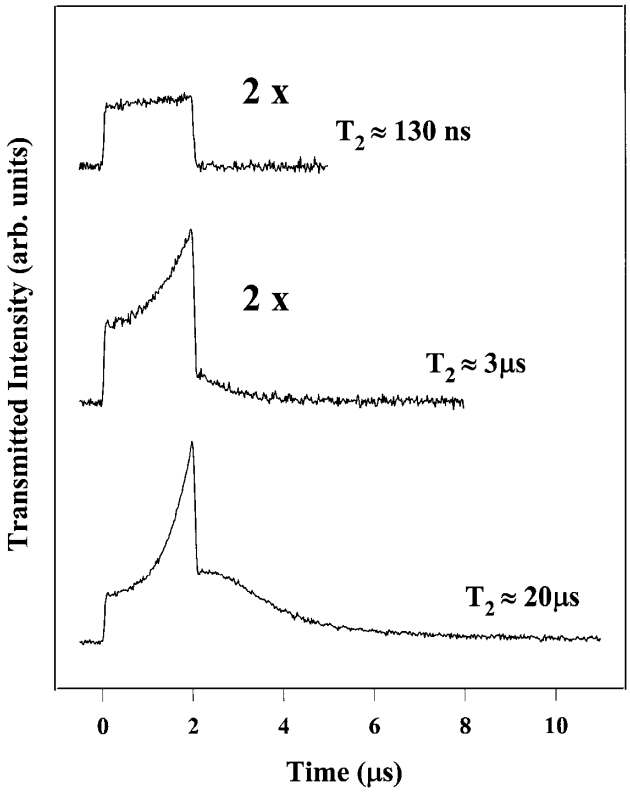

FIG. 5. Intensity transmitted through M2 versus time for different values of atomic coherence time T_2. $P_{\text{exc}} = 1.8$ mW; $0 < t < 2$ μs, excitation field on.

drives new internal atomic dynamics, including growth and decay of coherence.

In Fig. 5 we demonstrate that the superradiant decay process relies critically on atomic coherence. Each trace shown represents an average over seven single-event traces. Here, $P_{\text{exc}} = 1.8$ mW. From bottom to top in Fig. 5, the sample temperature was 4.6 K, 6 K, and 10 K, corresponding to homogeneous decoherence times of ~ 20 μs, ~ 3 μs, and ~ 130 ns, respectively. As the atoms decohere more rapidly the superradiant ringdown intensity is weaker and decays much faster (middle trace). When the atomic coherence time is short compared to the superradiant emission time of the lowest trace, no superradiant emission is observed.

In conclusion, we have reported the observation of optical superradiant ringdown in a regime relatively uncomplicated by material dephasing and the propagation effects found in optically thick single pass media. Cavity-assisted Dicke superradiant ringdown of our optically thin sample is observed following deterministic superradiant state preparation by pulsed coherent excitation. The cavity emission signal contains a significant fraction of the material excitation energy and is emitted in a time 2 orders of magnitude shorter than the incoherent spontaneous emission time. The experiment reported demonstrates a unique combination of the two methods of preparing superradiant states originally proposed by Dicke, i.e., coherent excitation followed by self-evolution to a maximally coherent state.

Note that the experimental system developed for this work uniquely provides an atomic-phase memory time that is 4 orders of magnitude longer than the cavity memory time. In this parameter regime, where $\tau_c < T_1, T_2$, one finds unique laser dynamics (type IV, class D laser behavior [10]) which has, through scarcity of appropriate systems, received little experimental scrutiny. The ability in our system of actively controlling T_2 through changes in sample temperature promises fertile opportunity to study unique regimes of laser operation as well as superradiance.

The authors thank Tsaipei Wang for helpful contributions. We appreciate support from the U.S. Air Force Office of Scientific Research under Contract No. F 49620-99-0214.

[1] R. H. Dicke, Phys. Rev. **93**, 99 (1954).
[2] N. Skribanowitz, I. P. Herman, J. C. MacGilivray, and M. S. Feld, Phys. Rev. Lett. **30**, 309 (1973); M. Gross, C. Fabre, P. Pillet, and S. Haroche, Phys. Rev. Lett. **36**, 1035 (1976); A. Flusberg, T. Mossberg, and S. R. Hartmann, Phys. Lett. **58A**, 373 (1976); H. M. Gibbs, Q. H. F. Vrehen, and H. M. J. Hikspoors, Phys. Rev. Lett. **39**, 547 (1977).
[3] R. Bonifacio and L. A. Lugiato, Phys. Rev. A **11**, 1507 (1975); Opt. Commun. **47**, 79 (1983).
[4] Reviews on the subject can be found in M. S. Feld and J. C. MacGillivray, in *Coherent Nonlinear Optics,* edited by M. S. Feld, and V. S. Letokhov (Springer, Berlin, 1980), p. 7; Q. H. F. Vrehen and H. M. Gibbs, in *Dissipative Systems in Quantum Optics,* Springer Topics in Current Physics Vol. 21, edited by R. Bonifacio (Springer, Berlin, 1982), p. 111; M. G. Benedict, A. M. Ermoloaev, V. A. Malyshev, I. V. Sokolov, and E. D. Trifonov, *Superradiance: Multiatomic Coherent Emission* (Institute of Physics Publishing, Bristol and Philadelphia, 1993).
[5] L. Allen and J. H. Eberly, *Optical Resonance and Two-Level Atoms* (Dover, New York, 1987).
[6] R. Friedberg and S. R. Hartmann, Phys. Lett. **37A**, 285 (1971).
[7] D. J. Heinzen, J. E. Thomas, and M. S. Feld, Phys. Rev. Lett. **54**, 677 (1985).
[8] Y. Kaluzny, P. Goy, M. Gross, J. M. Raimond, and S. Haroche, Phys. Rev. Lett. **51**, 1175 (1983).
[9] C. Greiner, B. Boggs, T. Loftus, T. Wang, and T. W. Mossberg, Phys. Rev. A **60**, 2657 (1999).
[10] N. A. Abraham, P. Mandel, and L. M. Narducci, *Dynamic Instabilities and Pulsations in Lasers,* Progress in Optics XXV, edited by E. Wolf (Elsevier, Amsterdam, 1988); Y. I. Khanin, *Principles of Laser Dynamics* (North-Holland, Amsterdam, 1995).